

Radiologe 2019 · 59 (Suppl 1):S10–S20
<https://doi.org/10.1007/s00117-019-0553-2>
 Published online: 6 June 2019
 © Springer Medizin Verlag GmbH, ein Teil von Springer Nature 2019



Patricia Leutz-Schmidt^{1,2,3} · Monika Eichinger^{1,2,3} · Mirjam Stahl^{2,4,6} ·
 Olaf Sommerburg^{2,4,6} · Jürgen Biederer^{1,2,3,9} · Hans-Ulrich Kauczor^{1,2,3,6} ·
 Michael U. Puderbach^{1,2,3,5} · Marcus A. Mall^{2,6,7,8} · Mark O. Wielpütz^{1,2,3}

¹ Department of Diagnostic and Interventional Radiology, Subdivision Pulmonary Imaging, University Hospital of Heidelberg, University of Heidelberg, Heidelberg, Germany

² Translational Lung Research Center Heidelberg (TLRC), German Lung Research Center (DZL), Heidelberg, Germany

³ Department of Diagnostic and Interventional Radiology with Nuclear Medicine, Thoraxklinik, University Hospital of Heidelberg, Heidelberg, Germany

⁴ Division of Pediatric Pulmonology & Allergy and Cystic Fibrosis Center, Department of Pediatrics, University of Heidelberg, Heidelberg, Germany

⁵ Department of Diagnostic and Interventional Radiology, Hufeland Hospital, Bad Langensalza, Germany

⁶ Department of Translational Pulmonology, University Hospital Heidelberg, Heidelberg, Germany

⁷ Department of Pediatric Pulmonology, Immunology and Intensive Care Medicine, Charité-Universitätsmedizin Berlin, Berlin, Germany

⁸ Berlin Institute of Health (BIH), Berlin, Germany

⁹ Faculty of Medicine, University of Latvia, Riga, Latvia

Ten years of chest MRI for patients with cystic fibrosis

Translation from the bench to clinical routine

Cystic fibrosis (CF) is the most common lethal autosomal-recessive disease in the White population [1]. The disease is caused by multiple, different mutations of the CF transmembrane conductance regulator (CFTR) protein, which acts as a Cl⁻ channel in epithelia such as the airways or intestinal glands and interacts with other epithelial ion channels such as the epithelial sodium channel ENaC. As a result, epithelial surface liquid is dehydrated and highly viscous secretions obstruct the conducting airways in particular. Chronic bacterial infection and inflammation subsequently destruct the airways and lung parenchyma, which can be assessed by imaging.

Lung imaging plays a central role in monitoring CF lung disease for all patient ages, as the lung manifestations determine morbidity and mortality despite improved understanding of the pathophysiology and improved therapy. As a result of improved management and care, CF patients are diagnosed early and retain a normal lung function for a longer period of time, and the majority of CF patients are now of adult age [2].

Two major advancements have further changed the management of CF patients in the past few years. First, newborn screening programs have been introduced in most Western countries and opened a unique window of opportunity to prevent or delay the irreversible progression of lung damage [3]. Second, a novel class of therapeutics has been developed, which may restore CFTR channel activity at least for some mutations.

Imaging has the potential to detect signs of regional lung disease long before lung function starts to be impaired, even in asymptomatic infants, and may thus offer new opportunities for early detection of regional lung disease and monitoring of disease activity. With imaging, lung changes may be differentiated into potentially reversible manifestations such as mucus plugging versus potentially irreversible manifestations such as bronchiectasis [4], both of which could be used for therapy control. Traditionally, chest radiography has been used to image the CF lung [5, 6]. Later, computed tomography (CT) was used in CF centers owing to its unparalleled spatial

resolution and thus higher sensitivity for airway changes, and it was shown that CT is more sensitive in predicting disease progression than forced expiratory volume in 1 s (FEV₁; [7]). Because this puts young, in particular, and thus susceptible patients at risk of cumulating ionizing radiation [8] through life-long surveillance imaging and image-guided procedures [8, 9], we sought to introduce chest magnetic resonance imaging (MRI) into CF imaging as a novel tool for lung imaging in research, as an endpoint for clinical trials, and, most importantly, as a robust routine modality with a focus on repeat surveillance imaging.

More than a decade ago, the chest was considered a black hole for MRI owing to well-known and, at that time, accepted limitations such as limited availability of protons to generate signal as well as fast signal decay due to air–tissue interfaces, and little work was available challenging this dogma [10]. In order to develop lung MRI into an alternative cross-sectional modality saving ionizing radiation and to harvest its additional potential for functional studies, we conducted studies

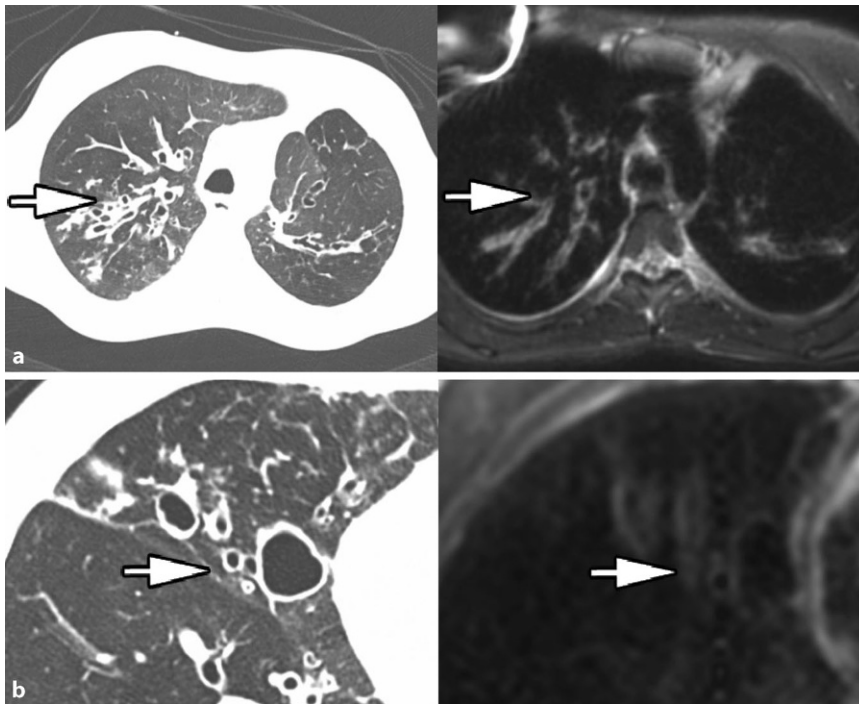


Fig. 1 ▲ Computed tomography (CT) and magnetic resonance imaging (MR) images of an 8-year-old female patient with cystic fibrosis (CF). Slices in comparable slice position: **a** inspiratory multislice computed tomography (MSCT), **b** T2 BLADE sequence. In the right lung, the CT and the MRI show bronchiectasis with mucus plugging (white arrows)

required to achieve this goal in the past few years.

Material and methods

Research agenda

A robust and vendor-independent morphofunctional MRI protocol had to be developed and implemented on clinical MRI scanners. A dedicated chest MRI scoring system for the semiquantitative evaluation of specific imaging findings had to be established. With this semiquantitative assessment, chest MRI was then cross-validated against CT as the standard of reference, as well as against plain film chest radiography, and also against established measurement techniques of lung function. Then, chest MRI could be employed in the target populations to describe the interindividual variation of the disease extent in a cross-sectional study. Next, the MRI protocol had to be expanded to multiple sites and validated in multicenter settings. To determine the sensitivity of MRI in detecting changes in disease severity, the protocol

was applied to patients with acute pulmonary exacerbation and was repeated after antibiotic therapy.

MRI scanner

For all of our studies, a clinical 1.5-T MRI scanner was used (Magnetom Symphony and Magnetom Avanto, Siemens Healthineers, Erlangen, Germany), unless stated otherwise.

Results

Development of a dedicated MRI protocol

With the introduction of parallel imaging, basic sequences could be adopted from abdominal MRI and adjusted to the requirements of lung imaging. Depending on patient age and cooperation, non-breath-hold and breath-hold acquisitions were implemented. Usually, the age of 6 years marks the point after which patients comply with breathing instructions. Before that age, patients were routinely sedated with 100 mg/kg chloral hy-

drate (maximum dose, 2 g/day), administered orally or rectally before the imaging procedure. Each MRI examination starts with a balanced steady-state free-precession sequence (bSSFP, TrueFISP) in free-breathing and in three planes. Then, each examination continues with T1-weighted sequences, either fast spin echo with averaging (TSE) in free breathing or three-dimensional (3D) gradient echo sequences (VIBE) in breath-hold, each in two planes, respectively. T2-weighted fast spin echo sequences with half-Fourier acquisition (HASTE) can be acquired in free-breathing using navigator techniques (PACE) or in breath-hold (Fig. 1).

Four-dimensional (4D) first-pass perfusion imaging was performed with a spoiled 3D gradient echo sequence with parallel imaging and echo sharing (“keyhole” sequence, TWIST). During multiple subsequent acquisitions of the perfusion series, gadolinium-based macrocyclic contrast material is injected intravenously by a power injector (0.1 mmol/kg body weight Gd-DOTA [Dotarem, Guerbet, Villepinte, France]) at an age-adjusted rate of 2–5 ml/s followed by a chaser of 30–50 ml NaCl 0.9% at the same injection rate. For an easy assessment, subtraction images are generated by subtracting the baseline images without contrast from those with maximum contrast in the lung parenchyma, displaying the maximum parenchymal enhancement. After perfusion imaging, T1-weighted imaging is repeated as postcontrast evaluation. The protocol can be readily transferred to other vendor platforms [11]. The pulse sequence parameters are shown in detail in Tables 1 and 2 for pediatric and adolescent/adult patients separately.

Developing a dedicated scoring system

Scoring systems allowing for a semiquantitative assessment of CF lung disease severity already existed for chest radiography (e.g., Chrispin–Norman chest score; [12]) and CT (e.g., Helbich [Bhalla] score, Brody score; [13, 14]). These are not suitable for MRI scoring because of a slightly different presen-

P. Leutz-Schmidt · M. Eichinger · M. Stahl · O. Sommerburg · J. Biederer · H.-U. Kauczor · M. U. Puderbach · M. A. Mall · M. O. Wielpütz

Ten years of chest MRI for patients with cystic fibrosis. Translation from the bench to clinical routine

Abstract

Background. Despite recent advances in our knowledge about the pathophysiology and treatment of cystic fibrosis (CF), pulmonary involvement remains the most important determinant of morbidity and mortality in patients with CF. Since lung function testing may not be sensitive enough for subclinical disease progression, and because young children may have normal spirometry results over a longer period of time, imaging today plays an increasingly important role in clinical routine and research for the monitoring of CF lung disease. In this regard, chest magnetic resonance imaging (MRI) could serve as

a radiation-free modality for structural and functional lung imaging.

Methods. Our research agenda encompassed the entire process of development, implementation, and validation of appropriate chest MRI protocols for use with infant and adult CF patients alike.

Results. After establishing a general MRI protocol for state-of-the-art clinical 1.5-T scanners based on the available sequence technology, a semiquantitative scoring system was developed followed by cross-validation of the method against the established modalities of computed tomography, radiography, and lung function testing. Cross-sectional studies

were then set up to determine the sensitivity of the method for the interindividual variation of the disease and for changes in disease severity after treatment. Finally, the MRI protocol was implemented at multiple sites to be validated in a multicenter setting.

Conclusion. After more than a decade, lung MRI has become a valuable tool for monitoring CF in clinical routine application and as an endpoint for clinical studies.

Keywords

Lung · Chest · Magnetic resonance imaging · Functional imaging · Validation

10 Jahre Thorax-MRT für Patienten mit zystischer Fibrose. Übertragung vom Versuchsstadium in die klinische Routine

Zusammenfassung

Hintergrund. Trotz aktueller Fortschritte im Wissen über die Pathophysiologie und Behandlung der zystischen Fibrose (CF) bleibt die Lungenbeteiligung die wichtigste Determinante für Morbidität und Mortalität bei Patienten mit CF. Da die Lungenfunktionsprüfung möglicherweise nicht empfindlich genug ist, subklinisches Fortschreiten der Erkrankung anzuzeigen, und weil kleine Kinder über einen längeren Zeitraum normale Spirometrieergebnisse aufweisen können, spielt heutzutage die Bildgebung eine immer wichtigeren Rolle im klinischen Alltags- und Wissenschaftsbetrieb zur Überwachung der Lungenbeteiligung bei CF. Hierbei könnte die Magnetresonanztomographie (MRT) des Thorax als strahlungsfreie Modalität zur struk-

turellen und funktionellen Lungenbildgebung dienen.

Methoden. Das Forschungsprogramm der Autoren umfasste den gesamten Ablauf der Entwicklung, Etablierung und Validierung gleichermaßen geeigneter Thorax-MRT-Protokolle zum Einsatz bei CF-Patienten im Kindes- wie im Erwachsenenalter.

Ergebnisse. Nach Etablierung eines allgemeinen MRT-Protokolls für den Stand der Technik entsprechende klinische 1,5-T-MRT-Geräte auf der Basis der verfügbaren Sequenztechnologie wurde ein semiquantitatives Punktesystem entwickelt mit anschließender Kreuzvalidierung der Methode gegen etablierte Verfahren wie Computertomographie, Röntgenuntersuchung und Lungenfunktionsprüfung. In Querschnittstudien wurde

dann die Sensitivität der Methode für die interindividuelle Variation der Erkrankung und für Veränderungen der Krankheitsschwere nach Behandlung ermittelt. Schließlich wurde das MRT-Protokoll an mehreren Einrichtungen etabliert, um es in einer Multizenterstudie zu validieren.

Schlussfolgerung. Nach mehr als einem Jahrzehnt ist die MRT zu einem wertvollen Instrument für die Überwachung der CF im klinischen Alltag und zu einem Endpunkt in klinischen Studien geworden.

Schlüsselwörter

Lunge · Thorax · Magnetresonanztomographie · Funktionelle Bildgebung · Validierung

tation of morphological abnormalities at MRI compared with CT. Furthermore, MRI, in comparison with CT, also provides functional information (contrast-enhanced lung perfusion imaging), which has to be integrated into an MRI score. This novel score should cover the morphological and also the functional changes in the CF lung, and reflect the wide range of disease severity from infancy to adulthood.

Thus, a novel CF MRI scoring system was developed that consists of six

subscores: (1) bronchiectasis/bronchial wall thickening, (2) mucus plugging, (3) abscesses/sacculations, (4) consolidations, (5) special findings (e.g., pleural reaction/effusion/pneumothorax), and (6) perfusion abnormalities (Table 3). Findings were evaluated for each lobe (lingua treated as own lobe) on a three-point scale as follows: 0 = no abnormality, 1 = <50% of the lobe is involved, 2 = ≥50% of the lobe is involved. The score proved to be reproducible for readers with experience in chest MRI, and

a reading time of 10 min may also be acceptable for clinical routine. Items 1–5 are summed up as the MRI morphology score, item 6 is the MRI perfusion score, and the sum of 1–6 amounts to the MRI global score. Global scores in 35 CF patients of a broad age range (mean age, 15.3 years; range, 0.5–42) were from 6 to 47. Intra- and inter-reader agreement for global scores were good, and concordance correlation coefficients (CCC) between two readers (R1 and R2) were: 0.98 (R1), 0.94 (R2), and 0.97 (R1/R2)

Table 1 MRI protocol for patients aged 0–6 years. From [21]

Sequence	Specials	Plane	TR (ms)	TE (ms)	ST (mm)	Distance factor (%)	Slices	FOV (mm ²)	Matrix	Voxel size (mm)	Scan time (min:s)
T1/2 bSSFP	–	Tra	339.40	1.26	4.0	–50	70	300×213	256×118	1.2×1.8	0:24
T1/2 bSSFP	–	Cor	381.44	1.42	4.0	–50	67	300×244	256×168	1.2×1.5	0:26
T1/2 bSSFP	–	Sag	337.00	1.26	4.0	–50	81	300×211	256×146	1.2×1.4	0:27
T1 FSE	4x averaging	Tra	450	9.5	4.0	10	24	300×178	512×243	0.6×0.7	2:29
T1 FSE	3x averaging	Cor	641	14	4.0	10	23	299×196	384×202	0.8×1.0	3:06
T2 FSE	Navigated	Tra	700	42	6.0	10	17	300×159	256×82	1.2×2.0	0:48
T2 FSE	Navigated	Cor	700	67	6.0	10	18	300×178	256×91	1.2×2.0	0:49
Perfusion	35 acquisitions, i.v. contrast	Cor	2.1	0.87	5.0	–	24	300×300	256×179	1.2×1.7	0:31
T1 FSE ce	4x averaging	Tra	450	9.5	4.0	10	24	300×178	512×243	0.6×0.7	2:29
T1 FSE ce	3x averaging	Cor	641	14	4.0	10	23	299×196	384×201	0.8×1.0	2:12

T1/2 bSSFP balanced T1/2-weighted steady-state free-precession sequence, *T1 FSE* T1-weighted fast spin echo sequence, *T2 FSE* T2-weighted single-shot fast spin echo with half-Fourier acquisition, *Perfusion* time-resolved 3D gradient echo sequence with parallel imaging and echo sharing for perfusion imaging acquired during contrast material injection (4D perfusion), *Tra* transversal plane, *Cor* coronary plane, *Sag* sagittal plane, *ce* contrast enhanced, *TR* repetition time, *TE* echo time, *ST* slice thickness, *FOV* field of view

Table 2 MRI protocol for patients aged ≥6 years

Sequence	Specials	Plane	TR (ms)	TE (ms)	ST (ms)	Distance factor (%)	Slices	FOV (mm ²)	Matrix	Voxel size (mm)	Scan time (min:s)
T1/2 bSSFP	–	Tra	290.30	1.21	4.0	–50	110	340×255	256×126	2.0×1.3	0:32
T1/2 bSSFP	–	Cor	318.40	1.16	4.0	–50	80	450×365	256×168	2.2×1.8	0:26
T1/2 bSSFP	–	Sag	318.40	1.16	4.0	–50	100	450×356	256×168	2.2×1.8	0:32
T1 GRE	Breath-hold	Tra	3.30	1.18	4.0	20	72	400×350	256×224	1.6×1.6	0:21
T1 GRE	Breath-hold	Cor	3.30	1.18	4.0	20	72	400×350	256×224	1.6×1.6	0:21
T2 FSE	Navigated or breath-hold	Tra	600	29	6.0	0	30	450×450	256×256	1.8×1.8	0:18
T2 FSE	Navigated or breath-hold	Cor	600	29	6.0	0	30	450×450	256×256	1.8×1.8	0:18
T2 blade	Navigated or multi-breath-hold	Tra	2700	116	4.0	15	42	400×400	320×320	1.3×1.3	4:28
T2 blade	Navigated or multi-breath-hold	Cor	2290	83	4.0	10	35	300×300	320×320	0.9×0.9	2:39
Perfusion	30 acquisitions, i.v. contrast	Cor	2.04	0.81	5.0	–	32	500×500	320×224	2.2×1.6	0:49
T1 GRE ce	Fat saturation	Tra	3.30	1.18	4.0	10	72	400×350	256×224	1.6×1.6	0:24
T1 GRE ce	Fat saturation	Cor	3.30	1.18	4.0	10	72	400×350	256×224	1.6×1.6	0:24

T1/2 bSSFP balanced T1/2-weighted steady-state free-precession sequence, *T1 GRE* T1 gradient echo sequence, *T2 FSE* T2-weighted single-shot fast spin echo with half-Fourier acquisition, *Perfusion* time-resolved 3D gradient echo sequence with parallel imaging and echo sharing for perfusion imaging acquired during contrast material injection (4D perfusion), *Tra* transversal plane, *Cor* coronary plane, *Sag* sagittal plane, *ce* contrast enhanced, *TR* repetition time, *TE* echo time, *ST* slice thickness, *FOV* field of view

(**Table 4**). There was no difference in CCC when comparing high and low scores [15].

Subsequently, the phenomenon of mosaic perfusion on T2-weighted MRI sequences in 50 infants and preschool children (mean age, 3.5±1.4 years; range, 0–6 years) was examined, and it was demonstrated that non-contrast-enhanced MRI reliably detects mosaic

signal intensity in infants and preschool children with CF, reflecting pulmonary blood volume distribution. The inter-reader agreement was also high (kappa = 0.71, 0.62–0.79; [16]).

Cross-validation against radiography, CT, and lung function

Initially, the modified Helbich (Bhalla) score for a direct comparison between MRI and CT was used, because this scoring system can be used for both modalities. A good correlation was seen between MRI and CT ($r=0.80$; $p<0.0001$) in 31 patients with stable lung disease

Table 3 Scoring sheet for morphofunctional MRI assessment. From [15]

	Right			Left			Maximal parameter/global score
	UL	ML	LL	UL	LG	LL	
1. Bronchiectasis/wall thickening	–	–	–	–	–	–	12
2. Mucus plugging	–	–	–	–	–	–	12
3. Abscesses/sacculations	–	–	–	–	–	–	12
4. Consolidations	–	–	–	–	–	–	12
5. Special findings	–	–	–	–	–	–	12
6. Perfusion size	–	–	–	–	–	–	12
Maximal lobar/global score	12	12	12	12	12	12	72

Findings were scored to be absent (0), within less than 50% of the lobe (1) or throughout more than 50% of the lobe (2). A global score and the following subscores were defined: global score (GS): sum of all parameters of the whole lung; maximum 72. Morphology score (MS): sum of morphological parameter scores (1–5) of the whole lung; maximum 60. Function score (FS): perfusion score (6) of the whole lung; maximum 12

UL upper lobe, ML middle lobe, LL lower lobe, LG lingula

Table 4 Intra- and inter-reader agreement for global morphology and functional score From [15]

Scores	Reader	MD	LLA	ULA	CCC	TDI (0.9)	CP (d)
Global	–	–	–	–	–	–	CP (8)
	R1 ^a	–0.48	–4.8	3.8	0.98	3.8	1.0
	R2 ^a	–1.7	–7.8	4.4	0.94	5.9	0.97
	R1/2 ^a	–0.3	–5	4.3	0.97	4	1.0
Morphology	–	–	–	–	–	–	CP (6)
	R1 ^a	–0.5	–3.9	2.9	0.98	3	1.0
	R2 ^a	–0.6	–5.9	4.7	0.94	4.6	0.96
	R1/2 ^a	–0.6	–3.8	2.5	0.98	2.8	1.0
Function	–	–	–	–	–	–	CP (2.5)
	R1 ^b	0.0	–2.9	2.9	0.89	2.5	0.9
	R2 ^b	–1.0	–4.6	2.5	0.67	3.5	0.75
	R1/2 ^b	–0.3	–3.2	3.8	0.80	3.0	0.82

Intra- and inter-reader agreement for global, morphology, and function scores, given as mean differences (MD), upper and lower limits of agreement (ULA, LLA), concordance correlation coefficients (CCC), total deviation index calculated for $p=0.9$ (TDI [0.9]), and coverage probability (CP [d]).

Different values of d were used according to the maximum score

R1 intra-reader agreement for reader 1, R2 intra-reader agreement for reader 2, R1/2 inter-reader agreement for both readers

^aGood agreement

^bAcceptable

(mean age, 16.7 years; range, 7–42 years). For the cross-correlation against chest radiography, these were scored using the Crispin–Norman scoring system, which revealed a moderate correlation between the CF MRI score and the radiography score ($r=0.63$; $p<0.01$) in this population [17, 18].

In a subsequent study performed to assess the sensitivity of MRI in detecting early lung disease in infants and preschool children, we used the dedicated CF MRI scoring system to compare MRI against

radiography in 35 infants and preschool children (mean age, 3.1 ± 2.1 years; range, 0–6 years). Here, only a moderate correlation ($r=0.46$; $p<0.05$) was detected between the MRI global score and chest radiography score, probably reflecting that MRI has a higher sensitivity for mild CF lung disease than radiography [19].

Next, the CF MRI score was correlated against the lung clearance index (LCI) as a measure of lung function in 97 infants, preschool and school-age children with CF (age range, 0–21 years).

The LCI correlated moderately with the MRI global score in infants and toddlers ($r=0.57$; $p<0.05$), and well in older children ($r=0.84$; $p<0.001$) with CF. Especially perfusion MRI as a single parameter also showed a moderate correlation ($r=0.45$; $p<0.05$) and a good correlation ($r=0.74$; $p<0.001$). Additionally, the CF MRI score was higher in patients chronically infected with *Pseudomonas aeruginosa* compared with patients who did not have a chronic infection with this pathogen ($p<0.001$; [20]).

Cross-sectional cohort of early CF lung disease

A cohort study of 50 children evaluated the potential of MRI to detect abnormal lung structure and perfusion in infants and preschool CF children (mean age, 3.1 ± 2.1 years; range, 0–6 years) in stable clinical condition ($n=40$). Bronchial wall thickening/bronchiectasis and mucus plugging were the most prevalent morphological abnormalities found from the first year of life in most patients with CF (mean MRI global score, 10.0 ± 4.0), but not in non-CF control subjects (0.0 ± 0.0 , $p<0.001$). Moreover, perfusion abnormalities were also present in most patients, even in the absence of morphological changes in a given lung lobe (mean MRI perfusion score, 3.5 ± 2.0 ; ■ Table 5; [19]).

Multicenter validation

Next, these activities were expanded and validated with the MRI protocol for infants and preschool children in a multicenter setting. For this purpose, a standardized chest MRI protocol was implemented in three CF centers and applied in clinical routine imaging, and the images of 42 infants and preschool children with stable lung disease (mean age, 3.2 ± 1.5 years; range, 0–6 years) were subsequently analyzed using a questionnaire for image quality and the CF MRI score. All MRI examinations (100%) achieved diagnostic image quality (■ Fig. 2). In only 6% of examinations was incomplete lung coverage observed, and in 6% artifacts were found, but were compensated by the re-

Table 5 Prevalence and subscores of structural lung change and perfusion deficits in infants and preschool children with cystic fibrosis according to age. From [19]

Age (years)		0	1	2	3	4	5	6	All
Number of subjects, n		8	7	6	5	7	3	4	40
Wall thickening/ bronchiectasis	Prevalence n (%)	8 (100)	7 (100)	6 (100)	5 (100)	5 (71)	3 (100)	3 (75)	37 (93)
	Subscore	4.8±0.8	6.0±1.0	7.5±2.0	8.5±3.0	6.0±3.5	5.0±0.5	4.0±1.5	5.5±1.5
Mucus plugging	Prevalence n (%)	6 (75)	3 (43)	3 (50)	3 (60)	5 (71)	2 (67)	3 (75)	25 (63)
	Subscore	0.8±0.5	0.0±0.5	0.3±0.5	0.5±0.5	0.5±0.5	1.0±0.5	3.5±3.0	0.5±0.5
Consolidation	Prevalence n (%)	0	1 (14)	2 (33)	1 (20)	1 (14)	0	0	5 (13)
	Subscore	0	0.0±0.0	0.0±0.0	0.0±0.0	0.0±0.0	0	0	0.0±0.0
Pleural reaction	Prevalence n (%)	1 (13)	2 (29)	1 (17)	2 (40)	2 (29)	1 (33)	1 (25)	10 (25)
	Subscore	0.0±0.0	0.0±0.0	0.0±0.0	0.0±0.0	0.0±0.0	0.0±0.0	0.0±0.0	0.0±0.0
Perfusion	Prevalence n (%)	4 (50)	6 (86)	6 (100)	5 (100)	6 (86)	3 (100)	4 (100)	34 (85)
	Score	0.5±3.0	1.0±2.5	3.0±1.5	5.5±2.0	4.0±2.5	4.0±1.5	5.3±1.8	3.5±2.0

maining sequences in all patients. Also, the range of the MRI score was similar across centers with a mean global MRI score of 13.3 ± 5.8 , showing that MRI as the only radiation-free imaging modality available for this purpose is feasible and delivers sufficient information [21].

Application for therapy monitoring

In order to detect its sensitivity for therapy-related changes, MRI was employed for patients with acute pulmonary exacerbation and repeated after completion of a course of antibiotics approximately 1 month later. In ten infants and preschool children (mean age, 3.1 ± 2.1 years; range, 0–6 years) the MRI morphology ($p < 0.01$), MRI perfusion ($p < 0.01$), and MRI global scores ($p < 0.001$) were significantly higher in patients with acute exacerbation compared with patients with stable CF lung disease. After antibiotic therapy, all three MRI scores were significantly reduced to a level comparable to stable lung disease: The MRI morphology score was reduced from 12.5 ± 2.0 to 8.0 ± 3.0 ($p < 0.01$), the MRI perfusion score was reduced from 6.0 ± 1.0 to 2.0 ± 1.0 ($p < 0.05$), and the MRI global score was reduced from 18.0 ± 2.0 to 12.0 ± 3.0 ($p < 0.05$; **Fig. 3**; [19]).

In an independent study with ten school-age children with acute pulmonary exacerbation (age range, 0.2–21.1 years), a similar finding was made: The MRI morphology score (20

vs. 12), MRI perfusion score (6 vs. 3), and MRI global score (28 vs. 17) were significantly reduced after antibiotic therapy ($p < 0.05$; **Fig. 4**; [20]).

Discussion

Although the idea of lung MRI and so-called plus pathologies was proposed in the late 1980s, its practice in clinical routine was not applicable at that time. Plus pathologies are diseases that lead to an increase in protons in the environment of otherwise low-proton lung tissue, which improve the conditions for a relatively selective depiction of lung disease against the dark background of a normal lung [22, 23]. The aim was to develop a robust and vendor-independent morpho-functional MRI protocol that could be implemented on clinical MRI scanners. With the advent of parallel imaging, MRI sequences became available, which allowed scanning of the whole chest in a breath-hold, or alternatively, which allowed for the application of triggering techniques [17, 18]. Another important contribution was the introduction of key-hole gradient echo sequences with echo sharing, which helped to bring functional imaging into the arena of routine application [24–29].

Apart from being a substitute for structural imaging with CT and the benefit of avoiding ionizing radiation, MRI now holds the added value of perfusion imaging in airway diseases. As a result of hypoxic pulmonary vasoconstriction

(HPV, formally known as the Euler–Liljestrand mechanism), airway obstruction with reduced oxygen delivery to the adjacent lung also leads to a reduction in blood delivery to the affected lung units [30]. This phenomenon is well-known from CT in the context of mosaicism [5, 16, 31], and can now directly be visualized by contrast-enhanced four-dimensional perfusion MRI as part of a routinely applicable vendor-independent protocol ([11]; **Tables 1 and 2**).

As a next step, a dedicated chest MRI scoring system for the semi-quantitative evaluation of specific imaging findings became necessary. This system was developed in a two-step approach, initially adapting an existing CT scoring system such as the Bhalla–Helbich score [13, 14] and subsequently validated the morphological findings against CT and radiography, based on scoring systems [17]. However, novel perfusion imaging needed to be integrated as well, and required the addition of a dedicated subscore, which then led to the compilation of a novel CF MRI scoring system [15]. It was shown that the inter-reader agreement for this scoring system is similar to established CT scoring systems (**Tables 3 and 4**). With this semi-quantitative assessment, chest MRI was then successfully cross-validated also against plain radiography [19]. As another validation step, it was shown that the MRI scores correlates well with the LCI in infants to adults with CF [20]. Importantly, the study also showed that patients chronically infected with *P.*

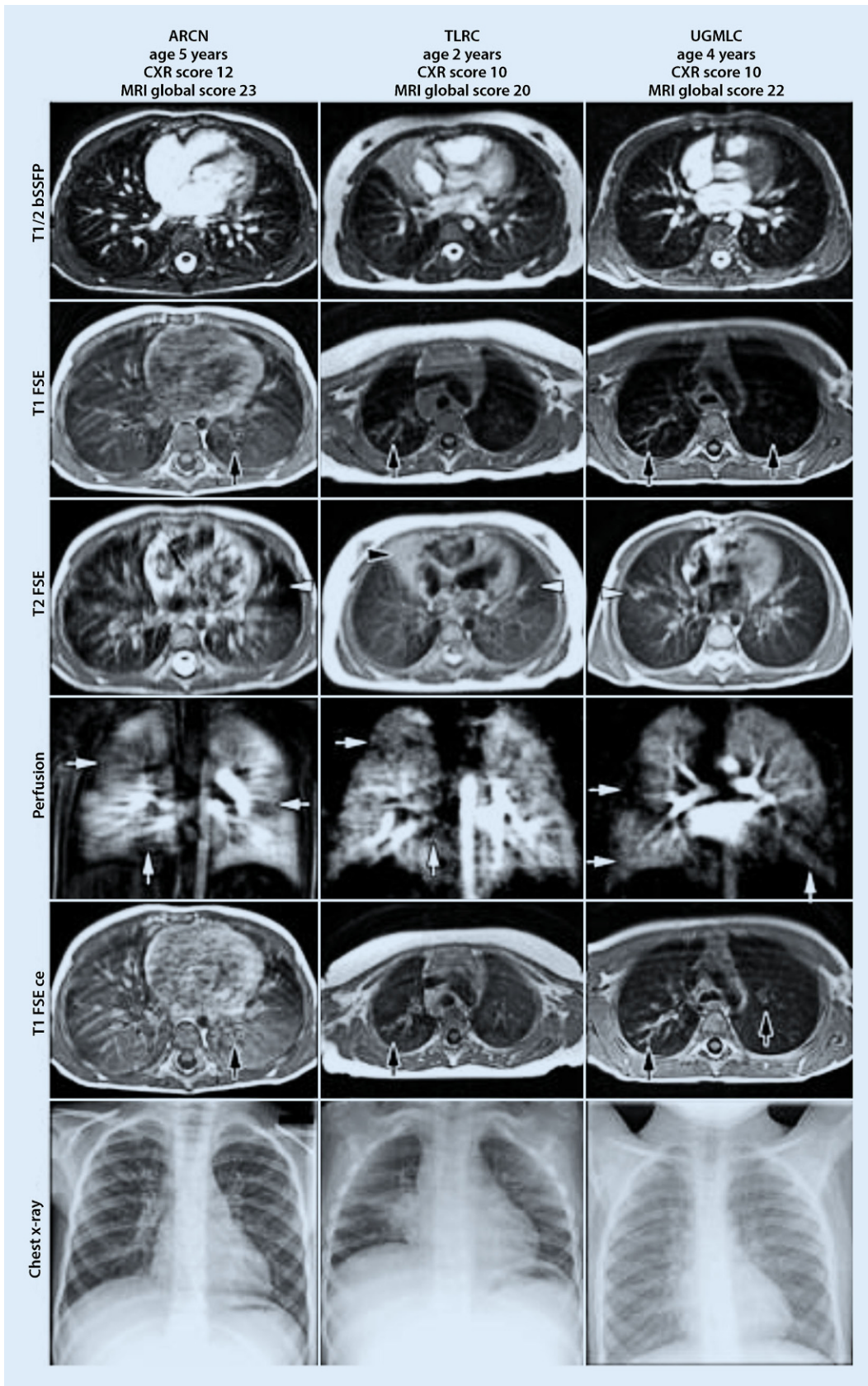


Fig. 2 ◀ Representative examples of the full lung magnetic resonance imaging (MRI) protocol in infants and preschool children with cystic fibrosis obtained at the three study sites matched by chest radiography (CXR) score. Patient age, CXR, and MRI scores are indicated on the top of the image. Airway wall thickening/bronchiectasis is best identified on T1-weighted images (black arrow) especially after contrast material injection (T1 FSE ce). Mucus plugging (white arrowhead), often associated with a mosaic pattern of hypointense lung parenchyma, and consolidations (black arrowhead) are best identified on T2-weighted images (T2 FSE). Perfusion abnormalities can be observed at all ages (white arrow, Perfusion). T1/2 bSSFP balanced T1/2-weighted steady-state free-precession sequence, T1 FSE T1-weighted fast spin echo sequence, T2 FSE T2-weighted single-shot fast spin echo with half-Fourier acquisition, Perfusion time-resolved 3D gradient echo sequence with parallel imaging and echo sharing for perfusion imaging acquired during contrast material injection (4D perfusion), ce contrast enhanced, ARCN Airway Research Center North, TLRC Translational Lung Research Center Heidelberg, UGMLC Universities of Giessen and Marburg Lung Center. (From [21])

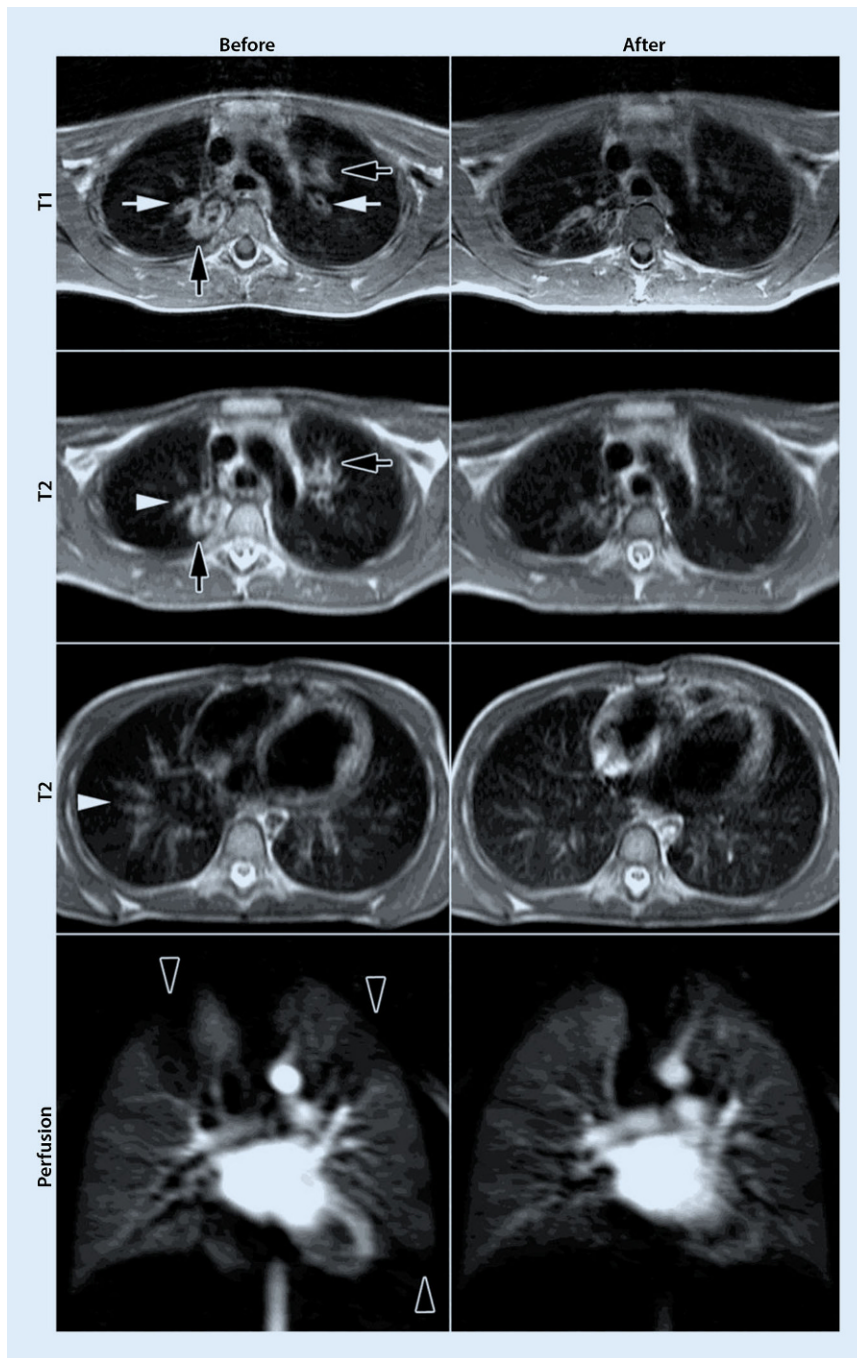


Fig. 3 ▲ Representative magnetic resonance imaging (MRI) studies of a 6-year-old patient with cystic fibrosis at the time of acute pulmonary exacerbation and 1 month after intravenous antibiotic therapy. The initial MRI study before treatment revealed extensive contrast-enhancing airway wall thickening (white arrows) and mucus plugging with high signal intensity on T2-weighted sequences (white arrowheads) of upper and lower lung lobes. Consolidations were present in both upper lobes (black arrows). Wedge-shaped perfusion abnormalities were identified on the subtracted perfusion map (black arrowheads). After antibiotic therapy, airway wall thickening and enhancement, mucus plugging, and consolidations were substantially reduced. Most perfusion defects resolved and a more homogeneous perfusion was restored. (From [19] Reprinted with permission of the American Thoracic Society. Copyright © 2019 American Thoracic Society. The *American Journal of Respiratory and Critical Care Medicine* is an official journal of the American Thoracic Society)

aeruginosa, which indicates a more advanced stage of CF lung disease, also have significantly higher MRI scores [20].

The established MRI protocol and scoring system were routinely employed in the target population of 50 infant and preschool CF patients, and used to describe inter-individual variation of the disease extent in a cross-sectional study [19]. Here, airway changes and mucus plugging were the most prevalent and most severe findings, and even perfusion abnormalities could be identified starting from infancy (Table 5). Although there was some increase in MRI scores with age, this was not statistically significant, most likely because patients included in this study were diagnosed clinically. Of note, non-CF healthy controls did not show a significant signal in MRI scores. Subsequently, 97 school-age to adult CF patients were also studied with the same protocol. In this expanded cohort, the correlation with age was more evident [20].

Using the aforementioned chest MRI protocol, a high level of diagnostic image quality was achieved in a multicenter setting including two other centers for pediatric CF patients [21]. Also, disease severity as determined by the MRI score was similar among these centers, and similar to our findings in a previous study [19, 21].

Finally, it was shown that MRI is sensitive to capturing response to antibiotic therapy for pulmonary exacerbation in two independent sets of ten preschool and school-age patients. Patients with pulmonary exacerbation have significantly more severe MRI findings compared with age-matched CF patients in a clinically stable condition, and after therapy, scores were then reduced to a level that was comparable to patients in stable clinical condition [19, 20].

Here, we present the steps in implementing MRI of the lung in CF patients. From multiple studies, we generated evidence that MRI detects lung abnormalities in children even in the first year of life, in the expected frequency and range of characteristic abnormalities known from studies based on CT [4], and that CF lung disease should therefore be monitored early. This agrees with the notion

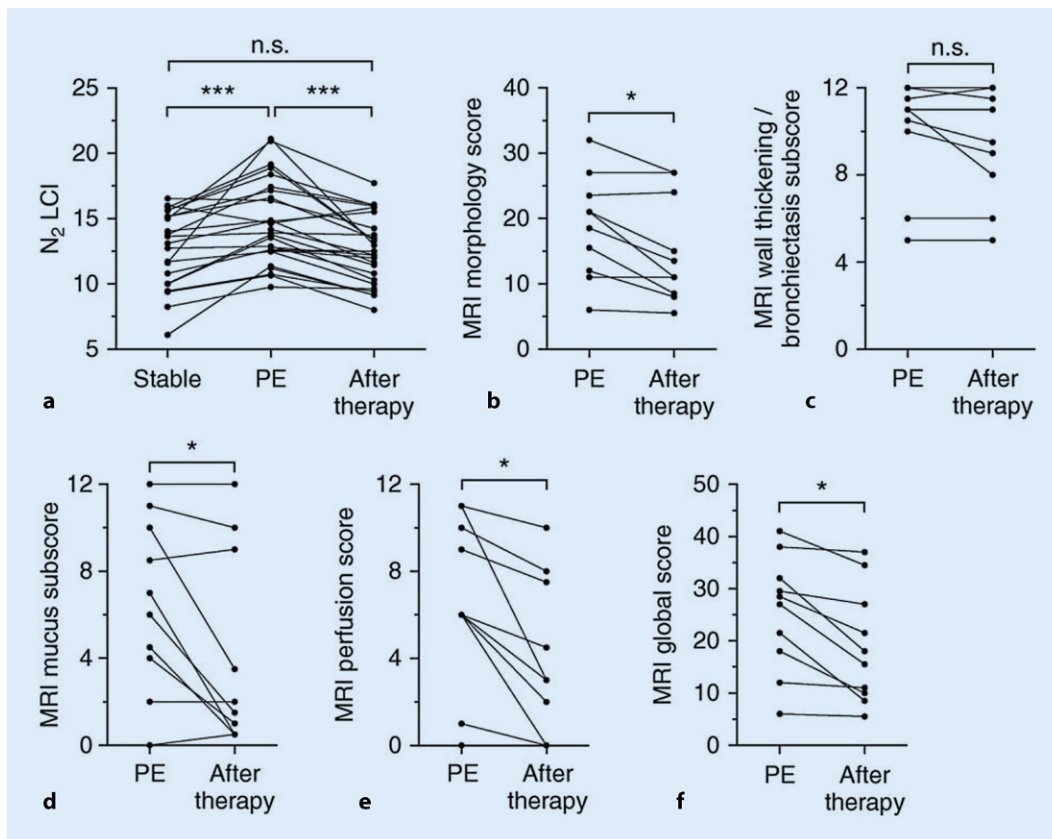


Fig. 4 ▲ Lung clearance index (LCI) and magnetic resonance imaging (MRI) detect response to antibiotic therapy of acute pulmonary exacerbations in children with cystic fibrosis (CF). **a** Nitrogen (N_2) LCI in children with CF at clinically stable baseline, at acute pulmonary exacerbation (PE), and after intravenous antibiotic therapy. **b–f** Summary of abnormalities in lung structure and perfusion detected by MRI in children with CF at acute PE and after intravenous antibiotic therapy. Data are shown for individual components of the MRI score, i.e., the morphology score (**b**), wall thickening/bronchiectasis subscore (**c**), mucus subscore (**d**), perfusion score (**e**), and the global MRI score (**f**). *Single asterisk: $p < 0.05$; Triple asterisk: $p < 0.001$. n.s.* not significant. (From [20] Reprinted with permission of the American Thoracic Society. Copyright © 2019 American Thoracic Society. The American Journal of Respiratory and Critical Care Medicine is an official journal of the American Thoracic Society)

that therapy needs to be enacted early in life, after identification through newborn screening [3, 5, 32, 33] in order to prevent or at least decelerate irreversible lung damage (Table 6).

Magnetic resonance imaging has several advantages over CT: It can provide additional functional information, e.g., perfusion imaging, in addition to structural information [8, 9] that cannot be assessed with CT routinely. Moreover, MRI is free of ionizing radiation and therefore can avoid the steady increase of radiation exposure due to medical interventions/diagnostic imaging especially in repeated surveillance imaging [34]. However, there are also disadvantages in lung imaging with MRI. Some are related to the use of gadolinium-based contrast material. We thus recommend to use macrocyclic contrast material. As

there are still debates about the deposition of gadolinium in human tissue, the clinical significance of which remains unknown [21, 30, 33, 35–38], developments toward non-contrast MRI such as Fourier decomposition MRI [39, 40] or T1-mapping [19, 20, 41] are welcome. Another implication of the longer acquisition times compared with CT is the need for sedation in infants and preschool children, which is routinely performed with chloral hydrate, and often allows for performing lung function measurements, e.g., LCI measurements, during the same sedation [42].

As an alternative to the proposed MRI protocol, several different functional MRI techniques in CF imaging have also been established and are available for scientific use so far: oxygen-enhanced MRI [43], hyperpolarized helium (^3He)-

MRI [39], and ^{129}Xe -MRI that, after the inhalation of gas, display only the ventilated airspace [44]. However, the cost of noble gas isotopes and also sophisticated technical prerequisites make these costly and rather unlikely to be introduced into broad clinical routine. Also, T1 relaxation time was used as an objective diagnostic parameter for pulmonary tissue [45], which can be combined with molecular oxygen to assess lung ventilation [46, 47]. Recently, ultra-short echo-time (UTE) MRI was introduced to overcome the problem of low spatial resolution, and high concordance to CT was demonstrated. Further, non-contrast-dependent proton MRI techniques

Table 6 Heidelberg scheme as a suggestion for longitudinal disease monitoring from birth. From [5]

	CXR	CT	MRI
Diagnosis screening <1 year	X	–	X (no CM)
Diagnosis >1 year	X	–	X
Annual follow-up <18 years	X	–	X
Annual follow-up ≥18 years	X	–	X
Clinical emergency	X	–	(X)
Emergency, hemorrhage	–	X (CM)	–

CM contrast material, CT computed tomography, CXR chest radiography, MRI magnetic resonance imaging

together with automated quantification will further reduce the need for contrast injection and user interaction, and will improve workflow [48, 49].

Practical conclusion

Radiation-free magnetic resonance imaging (MRI) today reliably detects a broad spectrum of severity in lung disease, ranging from early changes in lung structure and perfusion to advanced cystic fibrosis (CF) lung disease. This modality is sensitive to therapy response and is practicable in a multicenter setting with a high success rate, also with standardized vendor-independent protocols without radiation exposure. Proton MRI can now routinely be used for surveillance chest MRI in pediatric, adolescent, and adult patients with CF.

Corresponding address

Dr. med. Patricia Leutz-Schmidt

Department of Diagnostic and Interventional Radiology, Subdivision Pulmonary Imaging, University Hospital of Heidelberg, University of Heidelberg
Im Neuenheimer Feld 110, 69120 Heidelberg, Germany
Patricia.Leutz@med.uni-heidelberg.de

Funding. This study was supported in part by grants from the German Federal Ministry of Education and Research (82DZL00106, 82DZL001A6, 82DZL10201, 82DZL002A1, 82DZL00401, 82DZL004A1, 82DZL00501, 82DZL005A1). MAM was supported by the Einstein Foundation Berlin (EP-2017-393). ME, MUP, MS and MOW (C-H-P1504) received grants from the Christiane-Herzog-

Stiftung and the Mukoviszidose e. V., the German Cystic Fibrosis Foundation. ME was supported by the Mukoviszidose e. V. (S06/04 and S02/06) and the Deutsche Forschungsgemeinschaft (DFG MA 2081/4-1). MUP was supported by the Forschungsgemeinschaft Mukoviszidose (S06/04). MS was supported by Mukoviszidose e. V. (grant 15/01).

Compliance with ethical guidelines

Conflict of interest The funders had no role in the study design, data collection and analysis, decision to publish, or preparation of the manuscript. P. Leutz-Schmidt, M. Eichinger, M. Stahl, O. Sommerburg, J. Biederer, H.-U. Kauczor, M.U. Puderbach, M.A. Mall, and M.O. Wielputz declare no conflicts of interest related to this work.

For this article no studies with human participants or animals were performed by any of the authors. All studies performed were in accordance with the ethical standards indicated in each case.

The supplement containing this article is not sponsored by industry.

References

- Mall MA, Hartl D (2014) CFTR: cystic fibrosis and beyond. *Eur Respir J* 44:1042–1054
- Stern M, Wiedemann B, Wenzlaff P (2008) From registry to quality management: the German Cystic Fibrosis Quality Assessment project 1995–2006. *Eur Respir J* 31:29–35
- Sommerburg O, Stahl M, Hammermann J, Okun JG, Kulozik A, Hoffmann G, Mall M (2017) Newborn screening on cystic fibrosis in Germany: comparison of the new screening protocol with an alternative protocol. *Klin Padiatr* 229:59–66
- Sly PD, Gangell CL, Chen L, Ware RS, Ranganathan S, Mott LS, Murray CP, Stick SM (2013) Risk factors for bronchiectasis in children with cystic fibrosis. *N Engl J Med* 368:1963–1970
- Wielputz MO, Eichinger M, Biederer J, Wege S, Stahl M, Sommerburg O, Mall MA, Kauczor HU, Puderbach M (2016) Imaging of cystic fibrosis lung disease and clinical interpretation. *Rof* 188:834–845
- Cleveland RH, Stamoulis C, Sawicki G, Kelliher E, Zucker EJ, Wood C, Zurakowski D, Lee E (2014) Brasfield and Wisconsin scoring systems have equal value as outcome assessment tools of cystic fibrosis lung disease. *Pediatr Radiol* 44:529–534
- de Jong PA, Ottink MD, Robben SG, Lequin MH, Hop WC, Hendriks JJ, Pare PD, Tiddens HA (2004) Pulmonary disease assessment in cystic fibrosis: comparison of CT scoring systems and value of bronchial and arterial dimension measurements. *Radiology* 231:434–439
- Kuo W, Ciet P, Tiddens HA, Zhang W, Guillerman RP, van Straten M (2014) Monitoring cystic fibrosis lung disease by computed tomography. Radiation risk in perspective. *Am J Respir Crit Care Med* 189:1328–1336
- O’Connell OJ, McWilliams S, McGarrigle A, O’Connor OJ, Shanahan F, Mullane D, Eustace J, Maher MM, Plant BJ (2012) Radiologic imaging in cystic fibrosis: cumulative effective dose

and changing trends over 2 decades. *Chest* 141:1575–1583

- Kauczor HU, Heussel CP, Schreiber WG, Kreitner KF (2001) New developments in MRI of the thorax. *Radiologie* 41:279–287
- Biederer J, Beer M, Hirsch W, Wild J, Fabel M, Puderbach M, Van Beek EJ (2012) MRI of the lung (2/3). Why ... when ... how? *Insights Imaging* 3:355–371
- Weatherly MR, Palmer CG, Peters ME, Green CG, Fryback D, Langhough R, Farrell PM (1993) Wisconsin cystic fibrosis chest radiograph scoring system. *Pediatr Electron Pages* 91:488–495
- Bhalla M, Turcios N, Aponte V, Jenkins M, Leitman BS, McCauley DJ, Naidich DP (1991) Cystic fibrosis: scoring system with thin-section CT. *Radiology* 179:783–788
- Helbich TH, Heinz-Peer G, Eichler I, Wunderbaldinger P, Gotz M, Wojnarowski C, Brasch RC, Herold CJ (1999) Cystic fibrosis: CT assessment of lung involvement in children and adults. *Radiology* 213:537–544
- Eichinger M, Optazaita DE, Kopp-Schneider A, Hintze C, Biederer J, Niemann A, Mall MA, Wielputz MO, Kauczor HU, Puderbach M (2012) Morphological and functional scoring of cystic fibrosis lung disease using MRI. *Eur J Radiol* 81:1321–1329
- Leutz-Schmidt P, Stahl M, Sommerburg O, Eichinger M, Puderbach MU, Schenk JP, Alrajab A, Triphan SMF, Kauczor HU, Mall MA, Wielputz MO (2018) Non-contrast enhanced magnetic resonance imaging detects mosaic signal intensity in early cystic fibrosis lung disease. *Eur J Radiol* 101:178–183
- Puderbach M, Eichinger M, Haeselbarth J, Ley S, Kopp-Schneider A, Tuengerthal S, Schmaehl A, Fink C, Plathow C, Wiebel M, Demirakca S, Muller FM, Kauczor HU (2007) Assessment of morphological MRI for pulmonary changes in cystic fibrosis (CF) patients: comparison to thin-section CT and chest x-ray. *Invest Radiol* 42:715–725
- Puderbach M, Eichinger M, Gahr J, Ley S, Tuengerthal S, Schmaehl A, Fink C, Plathow C, Wiebel M, Muller FM, Kauczor HU (2007) Proton MRI appearance of cystic fibrosis: comparison to CT. *Eur Radiol* 17:716–724
- Wielputz MO, Puderbach M, Kopp-Schneider A, Stahl M, Fritzscheing E, Sommerburg O, Ley S, Sumkauskaitė M, Biederer J, Kauczor HU, Eichinger M, Mall MA (2014) Magnetic resonance imaging detects changes in structure and perfusion, and response to therapy in early cystic fibrosis lung disease. *Am J Respir Crit Care Med* 189:956–965
- Stahl M, Wielputz MO, Graeber SY, Joachim C, Sommerburg O, Kauczor HU, Puderbach M, Eichinger M, Mall MA (2017) Comparison of lung clearance index and magnetic resonance imaging for assessment of lung disease in children with cystic fibrosis. *Am J Respir Crit Care Med* 195:349–359
- Wielputz MO, von Stackelberg O, Stahl M, Jobst BJ, Eichinger M, Puderbach MU, Nahrlich L, Barth S, Schneider C, Kopp MV, Ricklefs I, Buchholz M, Tummeler B, Dopfer C, Vogel-Claussen J, Kauczor HU, Mall MA (2018) Multicentre standardisation of chest MRI as radiation-free outcome measure of lung disease in young children with cystic fibrosis. *J Cyst Fibros* 17:518–527
- Wielputz M, Kauczor HU (2012) MRI of the lung: state of the art. *Diagn Interv Radiol* 18:344–353
- Kauczor HUWMO (2018) MRI of the Lung. Springer, Berlin Heidelberg
- Fink C, Ley S, Risse F, Eichinger M, Zaporozhan J, Buhmann R, Puderbach M, Plathow C, Kauczor

- HU (2005) Effect of inspiratory and expiratory breathhold on pulmonary perfusion: assessment by pulmonary perfusion magnetic resonance imaging. *Invest Radiol* 40:72–79
25. Eichinger M, Puderbach M, Fink C, Gahr J, Ley S, Plathow C, Tuengerthal S, Zuna I, Muller FM, Kauczor HU (2006) Contrast-enhanced 3D MRI of lung perfusion in children with cystic fibrosis—initial results. *Eur Radiol* 16:2147–2152
 26. Kuder TA, Risse F, Eichinger M, Ley S, Puderbach M, Kauczor HU, Fink C (2008) New method for 3D parametric visualization of contrast-enhanced pulmonary perfusion MRI data. *Eur Radiol* 18:291–297
 27. Risse F, Eichinger M, Kauczor HU, Semmler W, Puderbach M (2011) Improved visualization of delayed perfusion in lung MRI. *Eur J Radiol* 77:105–110
 28. Eichinger M, Puderbach M, Heussel CP, Kauczor HU (2006) MRI in mucoviscidosis (cystic fibrosis). *Radiologe* 46:275–276, 278–281
 29. Ley S, Puderbach M, Risse F, Ley-Zaporozhan J, Eichinger M, Takenaka D, Kauczor HU, Bock M (2007) Impact of oxygen inhalation on the pulmonary circulation: assessment by magnetic resonance (MR)-perfusion and MR-flow measurements. *Invest Radiol* 42:283–290
 30. Hopkins SR, Wielputz MO, Kauczor HU (1985) Imaging lung perfusion. *J Appl Physiol* 113:328–339
 31. Stern EJ, Muller NL, Swensen SJ, Hartman TE (1995) CT mosaic pattern of lung attenuation: etiologies and terminology. *J Thorac Imaging* 10:294–297
 32. Sommerburg O, Hammermann J, Lindner M, Stahl M, Muckenthaler M, Kohlmüller D, Happich M, Kulozik AE, Stopsack M, Gahr M, Hoffmann GF, Mall MA (2015) Five years of experience with biochemical cystic fibrosis newborn screening based on IRT/PAP in Germany. *Pediatr Pulmonol* 50:655–664
 33. Mall MA, Stahl M, Graeber SY, Sommerburg O, Kauczor HU, Wielputz MO (2016) Early detection and sensitive monitoring of CF lung disease: prospects of improved and safer imaging. *Pediatr Pulmonol* 51:S49–S60
 34. Runge VM (2017) Critical questions regarding gadolinium deposition in the brain and body after injections of the gadolinium-based contrast agents, safety, and clinical recommendations in consideration of the EMA's Pharmacovigilance and risk assessment committee recommendation for suspension of the marketing authorizations for 4 linear agents. *Invest Radiol* 52:317–323
 35. Bauman G, Puderbach M, Deimling M, Jellus V, Chef'd'hotel C, Dinkel J, Hintze C, Kauczor HU, Schad LR (2009) Non-contrast-enhanced perfusion and ventilation assessment of the human lung by means of fourier decomposition in proton MRI. *Magn Reson Med* 62:656–664
 36. Bauman G, Puderbach M, Heimann T, Kopp-Schneider A, Fritzsche E, Mall MA, Eichinger M (2013) Validation of Fourier decomposition MRI with dynamic contrast-enhanced MRI using visual and automated scoring of pulmonary perfusion in young cystic fibrosis patients. *Eur J Radiol* 82:2371–2377
 37. Nyilas S, Bauman G, Pusterla O, Ramsey K, Singer F, Stranzinger E, Yammine S, Casaulta C, Bieri O, Latzin P (2018) Ventilation and perfusion assessed by functional MRI in children with CF: reproducibility in comparison to lung function. *J Cyst Fibros pii:S1569-1993(18)30854-3*. <https://doi.org/10.1016/j.jcf.2018.10.003>
 38. Kaireit TF, Sorrentino SA, Renne J, Schoenfeld C, Voskrebenezov A, Gutberlet M, Schulz A, Jakob PM, Hansen G, Wacker F, Welte T, Tümmler B, Vogel-Claussen J (2017) Functional lung MRI for regional monitoring of patients with cystic fibrosis. *PLoS ONE* 12:e187483
 39. Triphan SM, Jobst BJ, Breuer FA, Wielputz MO, Kauczor HU, Biederer J, Jakob PM (2015) Echo time dependence of observed T1 in the human lung. *J Magn Reson Imaging* 42:610–616
 40. Jobst BJ, Triphan SM, Sedlaczek O, Anjorin A, Kauczor HU, Biederer J, Ley-Zaporozhan J, Ley S, Wielputz MO (2015) Functional lung MRI in chronic obstructive pulmonary disease: comparison of T1 mapping, oxygen-enhanced T1 mapping and dynamic contrast enhanced perfusion. *PLoS ONE* 10:e121520
 41. Stahl M, Wielputz MO, Kauczor HU, Mall MA (2018) Reply to Verbanck and Vanderhelst: the respective roles of lung clearance index and magnetic resonance imaging in the clinical management of patients with cystic fibrosis. *Am J Respir Crit Care Med* 197:410–411
 42. Heidemann RM, Griswold MA, Kiefer B, Nittka M, Wang J, Jellus V, Jakob PM (2003) Resolution enhancement in lung 1H imaging using parallel imaging methods. *Magn Reson Med* 49:391–394
 43. Mentore K, Froh DK, de Lange EE, Brookeman JR, Paget-Brown AO, Altes TA (2005) Hyperpolarized HHe 3 MRI of the lung in cystic fibrosis: assessment at baseline and after bronchodilator and airway clearance treatment. *Acad Radiol* 12:1423–1429
 44. Smith L, Marshall H, Aldag I, Horn F, Collier G, Hughes D, West N, Horsley A, Taylor CJ, Wild J (2018) Longitudinal assessment of children with mild cystic fibrosis using hyperpolarized gas lung magnetic resonance imaging and lung clearance index. *Am J Respir Crit Care Med* 197:397–400
 45. Jakob PM, Wang T, Schultz G, Hebestreit H, Hebestreit A, Hahn D (2004) Assessment of human pulmonary function using oxygen-enhanced T(1) imaging in patients with cystic fibrosis. *Magn Reson Med* 51:1009–1016
 46. Ohno Y, Koyama H, Yoshikawa T, Seki S, Takenaka D, Yui M, Lu A, Miyazaki M, Sugimura K (2016) Pulmonary high-resolution ultrashort TE MR imaging: Comparison with thin-section standard- and low-dose computed tomography for the assessment of pulmonary parenchyma diseases. *J Magn Reson Imaging* 43:512–532
 47. Wielputz MO, Triphan SMF, Ohno Y, Jobst BJ, Kauczor HU (2018) Outracing lung signal decay—potential of Ultrashort echo time MRI. *Rof* 191(5):415–423. <https://doi.org/10.1055/a-0715-2246>
 48. Kaireit TF, Voskrebenezov A, Gutberlet M, Freise J, Jobst B, Kauczor HU, Welte T, Wacker F, Vogel-Claussen J (2019) Comparison of quantitative regional perfusion-weighted phase resolved functional lung (PREFUL) MRI with dynamic gadolinium-enhanced regional pulmonary perfusion MRI in COPD patients. *J Magn Reson Imaging* 49:1122–1132
 49. Fischer A, Weick S, Ritter CO, Beer M, Wirth C, Hebestreit H, Jakob PM, Hahn D, Bley T, Kostler H (2014) SELF-gated Non-Contrast-Enhanced FUnctional Lung imaging (SENCEFUL) using a quasi-random fast low-angle shot (FLASH) sequence and proton MRI. *NMR Biomed* 27:907–917